Molecular Microbiology (2009) 74(1), 209–226 ■
doi:10.1111/j.1365-2958.2009.06862.x
First published online 11 September 2009

Interconvertibility of lipid- and translocon-bound forms of the bacterial Tat precursor pre-SufI

Umesh K. Bageshwar, Neal Whitaker, Fu-Cheng Liang and Siegfried M. Musser*
Department of Molecular and Cellular Medicine, College of Medicine, Texas A&M Health Science Center, College Station, TX 77843, USA.

Summary

Signal peptides target protein cargos for secretion from the bacterial cytoplasm. These signal peptides contain a tri-partite structure consisting of a central hydrophobic domain (h-domain), and two flanking polar domains. Using a recently developed *in vitro* transport assay, we report here that a central h-domain position (C17) of the twin arginine translocation (Tat) substrate pre-SufI is especially sensitive to amino acid hydrophobicity. The C17I mutant is transported more efficiently than wild type, whereas charged substitutions completely block transport. Transport efficiency is well-correlated with Tat translocon binding efficiency. The precursor protein also binds to non-Tat components of the membrane, presumably to the lipids. This lipid-bound precursor can be chased through the Tat translocons under conditions of high proton motive force. Thus, the non-Tat bound form of the precursor is a functional intermediate in the transport cycle. This intermediate appears to directly equilibrate with the translocon-bound form of the precursor.

Introduction

There are two major protein transport systems in *Escherichia coli* that translocate proteins from the cytoplasm to the periplasm. The Sec machinery exports the majority of secretory proteins. This transport system translocates unfolded polypeptides in a linear fashion from N- to C-terminus. A minimal system consists of the SecYEG complex, which comprises the transmembrane pore, SecA, an ATPase that guides the signal peptide to and through the SecYEG translocon, and SecB, a chaperone that maintains the precursor in a transport competent configuration (Rusch and Kendall, 2007; Driessen and Nouwen, 2008). In contrast, the twin-arginine translocation (Tat) machinery exports fully folded and assembled proteins. A minimal system consists of the TatA, TatB and TatC membrane proteins (Sargent, 2007; Natale *et al.*, 2008). A dominant model is that TatBC oligomers act as receptors for the precursor protein, and TatA oligomers form ring-like structures, which provide the pore for passage of the folded cargo proteins (De Leeuw *et al.*, 2001; Gohlke *et al.*, 2005; Dabney-Smith *et al.*, 2006). In *E. coli*, approximately two-thirds of Tat substrates contain metalloprosthetic groups, which are inserted into the proteins in the cytoplasm (Papish *et al.*, 2003; Berks *et al.*, 2005; Matos *et al.*, 2008). Both Sec and Tat transport systems facilitate protein movement across the phospholipid membrane barrier without causing the collapse of transmembrane ion gradients, which are necessary for numerous physiological functions. In fact, a proton motive force (PMF) is the only energy source required for Tat transport. In *E. coli*, only one component of the PMF, the electric field gradient ($\Delta\psi$), appears essential for Tat transport – a ΔpH requirement has not been detected (Bageshwar and Musser, 2007). In contrast, ATP is essential for Sec-dependent transport. However, Sec transport efficiency is significantly enhanced by a PMF (Natale *et al.*, 2008; Liang *et al.*, 2009).

A typical signal peptide for both the Sec and Tat systems is comprised of three distinct domains – the n-domain, the h-domain and the c-domain. The n-domain is located at the extreme N-terminal end of the signal peptide, and is usually hydrophilic and often contains positively charged residues. The h-domain follows the n-domain, and is predominantly comprised of hydrophobic residues. The h-domain of Tat signal peptides are somewhat less hydrophobic and generally longer than those found in Sec signal peptides (Berks *et al.*, 2003; Bendtsen *et al.*, 2005; Shanmugham *et al.*, 2006). Numerous studies indicate that hydrophobic residues within the h-domain are important for promoting binding and transport (Chaddock *et al.*, 1995; Stanley *et al.*, 2000; Cline and Mori, 2001; Gérard and Cline, 2006; 2007; Li *et al.*, 2006). The polar c-domain is located at the C-terminal end of the signal peptide. Signal peptidase cleaves the signal peptide from the precursor protein after transport releasing the mature protein (Natale *et al.*,

Accepted 19 August, 2009. *For correspondence. E-mail smusser@tamu.edu; Tel. (+1) 979 862 4128; Fax (+1) 979 847 9481.

2008). The major difference between Sec and Tat signal peptides is the presence of a twin-arginine-containing consensus motif (which in bacteria is (S/T)-R-R-x-F-L-K) at the interface between the n- and h-domains of Tat presequences (Berks, 1996). In this consensus motif, the two arginines are almost invariant and virtually essential for efficient Tat transport, although natural exceptions occur in which lysine occurs in place of the first arginine (Hinsley *et al.*, 2001; Molik *et al.*, 2001).

The precise manner in which signal peptides promote cargo transport is not fully understood. As mentioned earlier, SecA and SecB are general and necessary chaperones for secretory proteins targeted to the Sec pathway. No general and necessary chaperones are known for the Tat system, at least not any displaying the broad specificity and essentiality as SecA and SecB within the Sec system. While SlyD and DnaK bind to multiple Tat precursor proteins, and thus could be considered 'general chaperones', they are not required for all precursor proteins (Oresnik *et al.*, 2001; Brüser *et al.*, 2003; Graubner *et al.*, 2007). Further, the deletion of SlyD has no effect *in vivo* (Graubner *et al.*, 2007). Efficient *in vitro* transport of pre-SufI does not require any chaperones (Bageshwar and Musser, 2007; Holzapfel *et al.*, 2009), suggesting that not all Tat substrates require chaperones. However, specific signal peptide binding chaperones, do exist, e.g. DmsD for DmsA (Oresnik *et al.*, 2001), NapD for NapA (Maillard *et al.*, 2007), HybE for HybO (Dubini and Sargent, 2003), and TorD for TorA (Jack *et al.*, 2004). In some cases, these chaperones appear necessary for a 'proof-reading' function (Jack *et al.*, 2004; Maillard *et al.*, 2007). The proposed role of this 'proof-reading' function is to ensure that only completely folded and assembled proteins are allowed to access the Tat export system (Bendtsen *et al.*, 2005; Berks *et al.*, 2005).

In the absence of a chaperone or after a chaperone has dissociated, signal peptide interactions with the membrane lipids may play a significant role in the translocation process. Based on the finding that thylakoid Tat precursors and *E. coli* Tat pre-sequences bind to pure lipid membranes, multiple investigators have postulated that signal peptide interactions with the membrane lipids may precede the interactions with translocon components, i.e. the precursor can two-dimensionally search for translocons from a lipid-bound state (Musser and Theg, 2000; Hou *et al.*, 2006; Shanmugham *et al.*, 2006). Consistent with this hypothesis, Tat substrates bind to Tat-deficient bacterial membranes (Sargent *et al.*, 1999; Bolhuis *et al.*, 2001; Brüser *et al.*, 2003). Protease treatment of membrane-bound Tat substrates yields fragments similar in size to the signal sequences, consistent with the hypothesis that an early step of the transport process is that the signal sequence becomes embedded in the membrane lipids and thus protected from proteases (Brüser *et al.*, 2003; Hou *et al.*, 2006). In a review on the membrane bilayer interactions of Tat signal sequences, it was suggested that this lipid interaction step could be crucial for the proof-reading function of the Tat pathway (Brüser and Sanders, 2003).

In our efforts to construct a cysteine-free signal peptide for pre-SufI, we discovered that the hydrophobicity of the residue at position C17, in the middle of the h-domain, strongly influences the membrane binding and transport promoting ability of this signal peptide. Pre-SufI binds to TatABCDE-deficient membranes, indicating the presence of non-Tat binding sites. At a high membrane potential, precursor bound to the non-Tat binding sites of TatABC-containing membranes was transported, suggesting that this non-Tat membrane-bound state is a functional intermediate in the transport process.

Results

Quantification of Tat and non-Tat interactions

As we reported earlier (Bageshwar and Musser, 2007), inverted membrane vesicles (IMVs) constructed from the *E. coli* strains MC4100 and JM109 are both suitable for measuring *in vitro* Tat transport activity. However, IMVs from the MC4100 strain yield lower transport efficiencies, on average, and the results are more variable. Thus, we used IMVs from the JM109 strain to determine transport efficiencies. However, there is no currently available TatABCDE deletion strain generated from JM109. Thus, to compare the membrane binding activity of precursors in the presence and absence of Tat translocons, we used IMVs from the MC4100 and MC4100ΔTatABCDE strains, respectively. Both our JM109 and MC4100 strains contained a TatABC overexpression plasmid (pTatABC; see *Experimental procedures*). IMVs constructed from the JM109 (pTatABC), MC4100 (pTatABC) and MC4100ΔTatABCDE strains are denoted pTat*, pTat and ΔTat respectively. For most of the experiments reported here, we used the natural Tat substrate pre-SufI.

Membrane binding activity was determined by incubating precursors with IMVs for 10 min at 37°C and then centrifuging the samples. The IMV pellets were washed, and then assayed by SDS-PAGE and Western blotting for the presence of precursor protein. TatABC-enriched IMVs from MC4100 and JM109 contained comparable amounts of TatA, TatB and TatC (Fig. S1A) and yielded similar ratios of inside-out vesicles (≥ 95%; Fig. S1B), in agreement with previous results (Bageshwar and Musser, 2007). These IMVs also exhibited similar binding capacities towards pre-SufI over a range of precursor concentrations (Fig. 1A). These data suggest that precursor interactions with IMVs from JM109 and MC4100 strains are similar, and therefore, that transport efficiency

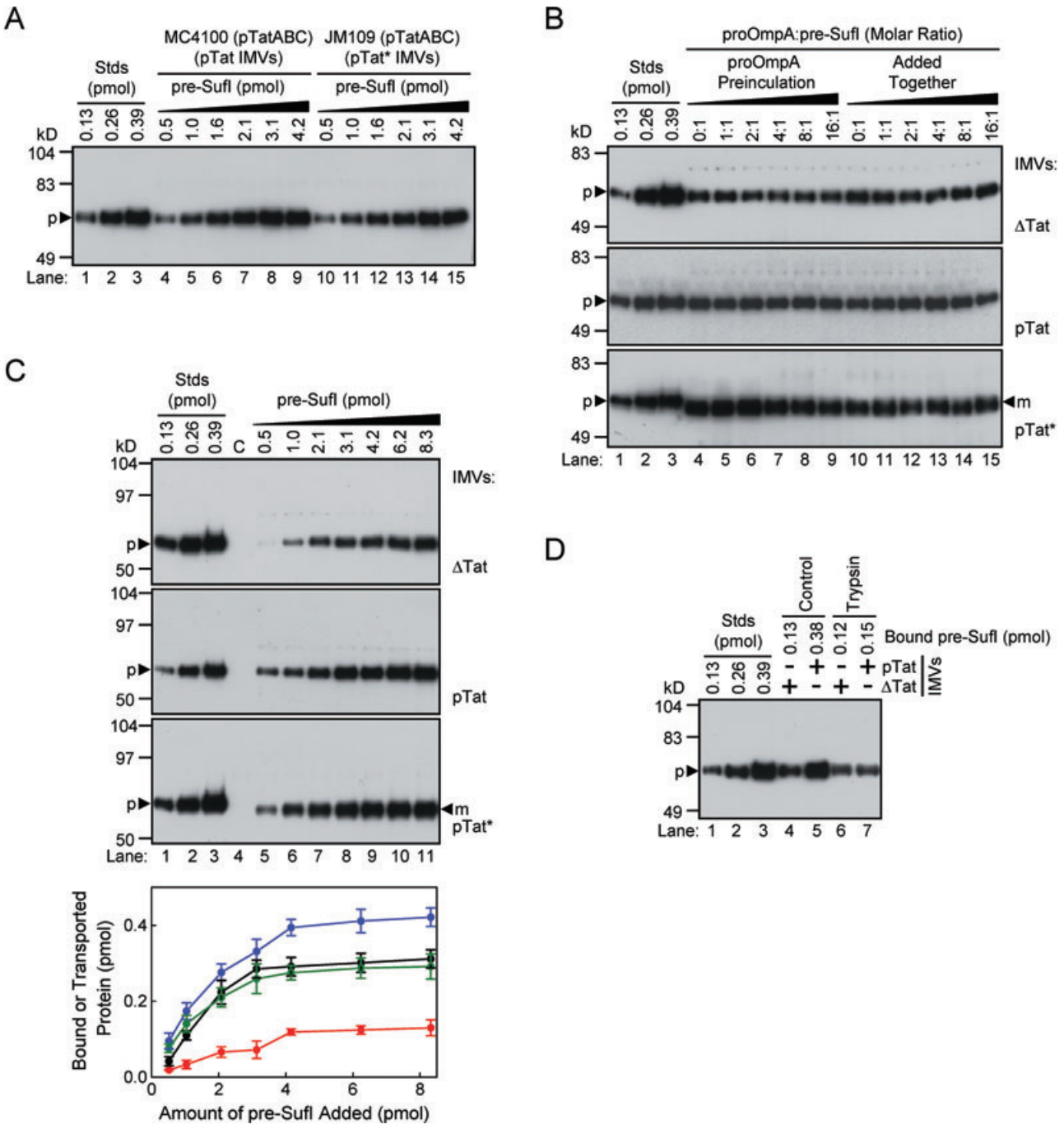

Fig. 1. Quantification of precursor–lipid and precursor–translocon interactions. All gels in this figure are anti-SufI immunoblots.
A. Membrane binding assay. The indicated amounts of pre-SufI were incubated with pTat or pTat* IMVs at pH 8.0 and then sedimented. The gel shows the amount of precursor protein recovered in the washed pellet fraction. Lanes 1–3 are quantification standards.
B. Competition between Sec and Tat precursors. Shown is the amount of membrane-bound (top and middle) and transported (bottom) pre-SufI in the presence of various molar equivalents of proOmpA-HisC. The proOmpA-HisC protein was pre-incubated with IMVs for 10 min prior to pre-SufI addition (lanes 4–9), or simultaneously with pre-SufI (lanes 10–15). Transport reactions were initiated with 4 mM NADH. Each lane contains the Sec chaperone SecB (25 μM).
C. Concentration dependence of membrane binding and transport. The binding of pre-SufI to ΔTat (top) and pTat (middle) IMVs was assayed as in A (pH 8.0). Transport into pTat* IMVs (bottom) was initiated by the addition of 4 mM NADH. Control lanes are devoid of pre-SufI for the binding assays, or with 8.3 pmol pre-SufI but no NADH for the transport assay. The plot shows the quantification of the pre-SufI bound to non-translocon components of the membrane (ΔTat IMVs, red), the pre-SufI bound to both Tat translocons and non-Tat membrane component (pTat IMVs, blue), and the pre-SufI transported into pTat* IMVs (black) ($n = 3$). The amount of pre-SufI bound to TatABC (green) was estimated by subtracting the red curve from the blue curve.
D. Binding to trypsin-treated IMVs. Membrane binding interactions were assayed as in A.

measurements with the JM109 strain can be reasonably interpreted in light of membrane binding interactions with MC4100 strains. Because of the different strains used for binding and transport, some differences (errors) are expected when comparing the absolute amounts of protein bound or transported. For this reason, we compare general trends instead of amounts. The membrane binding activity and transport efficiency of pre-SufI were not affected by up to a 16-fold molar excess of the Sec substrate proOmpA (Fig. 1B). Therefore, the Tat pathway is highly selective for the pre-SufI pre-sequence under the conditions described here. More importantly, the membrane binding activity shown towards ΔTat IMVs cannot be explained by the binding of pre-SufI to the Sec transport system.

The membrane binding activity and transport efficiency of pre-SufI depended upon the precursor concentration. Not surprisingly, TatABC-containing membranes had a higher precursor binding capacity than TatABC-deficient membranes. Assuming that the amount of non-Tat-bound precursor protein was identical for both types of membranes, the amount of precursor bound to the Tat transport machinery was estimated by subtracting the amount of precursor bound to Tat-deficient membranes from that bound to Tat-containing membranes. About twice as much wild-type pre-SufI binds to the Tat transport machinery as binds to non-translocon components (Fig. 1C). Thus, a significant fraction of pre-SufI does not bind directly to the Tat machinery. Interestingly, the amount of pre-SufI transported in the presence of NADH was almost indistinguishable from the amount of Tat translocon-bound precursor (Fig. 1C). These data suggest, at least for these conditions, that only pre-SufI bound to the Tat machinery can be chased into the IMV lumen by the addition of NADH. Both translocon binding and transport activity saturated at ~3–4 pmol pre-SufI. To maximize the total amount of bound precursor (total observable signal) and minimize the amount of unbound precursor that needs to be removed before analysis (as a percent of the total), 3.1 pmol (90 nM) pre-SufI was used for most of the subsequent experiments.

Pre-SufI binds to trypsin-treated membranes

To investigate whether pre-SufI binds to a non-Tat proteinaceous receptor, IMVs were treated with trypsin to digest proteins that might act as receptors. This protease digestion treatment was effective because translocon binding activity was eliminated from Tat-containing membranes. Pre-SufI binding to ΔTat membranes was unaffected by trypsinization (Fig. 1D), suggesting that binding was mediated by a non-protein membrane component. For simplicity, we will refer to the pre-SufI that binds to ΔTat IMVs as lipid-bound precursor. We do recognize, however, that trypsinization of IMVs may not have eliminated a non-Tat proteinaceous receptor.

Effects of chemical agents on membrane binding and transport

We next investigated the dependence of pre-SufI membrane binding activity and transport efficiency on pH, ionic strength and urea concentration (Fig. 2). We first discuss the observed pH effects (Fig. 2A). The effect of buffer pH on the ability of pre-SufI to bind to Tat translocons was significantly different from its effect on pre-SufI interactions with the membrane lipids. The lipid interactions were diminished by increased pH. The data are consistent with the hypothesis that binding is inhibited by a single deprotonation step at an apparent pK_a of ~7.5. In contrast, the Tat machinery interactions were optimal at pH ~8, consistent with protonation/deprotonation of the precursor and/or the Tat machinery on either side of this optimum. The transport efficiency also was optimal at pH ~8. This makes intuitive sense, considering that the precursor must bind to the Tat translocon before it can be transported. When transport was energetically driven by NADH addition, the amount of precursor transported was similar to the amount of translocon-bound precursor. This result is consistent with the hypothesis that NADH induces a single round of Tat turnover (Bageshwar and Musser, 2007). However, in the presence of ATP, a larger amount of precursor were transported than was found bound to Tat translocons, suggesting that additional pre-SufI must bind to Tat translocons during ATP-driven transport. This result is consistent with our previous conclusion that ATP maintains a stable, high magnitude PMF across the membrane, and thereby is capable of driving multiple turnover events (Bageshwar and Musser, 2007).

Variations in salt concentrations are typically used to identify the role of ionic interactions, an approach we used

Fig. 2. Effects of chemical agents and the RR → KK mutation on membrane binding and transport of pre-SufI. All gels in this figure are anti-SufI immunoblots.
A. Effect of pH on binding and transport efficiency. Shown is the effect of pH on pre-SufI binding (top), and on transport in the presence of 4 mM ATP with an ATP regenerating system (middle) or 4 mM NADH (bottom). The data were quantified as in Fig. 1C: (blue) precursor bound to pTat IMVs, (red) lipid-bound precursor, (green) translocon-bound precursor, (black, solid) precursor transported with NADH, and (black, open circles) precursor transported with ATP ($n = 3$).
B. Effect of KCl concentration on binding and transport efficiency. Key as in A ($n = 3$).
C. Effect of KK substitution for the RR motif (pre-SufI-KK-CCC) on pre-SufI binding and transport efficiency (Tr) ($n = 3$).
D. Effect of urea concentration on binding and transport efficiency. Key as in A ($n = 3$).

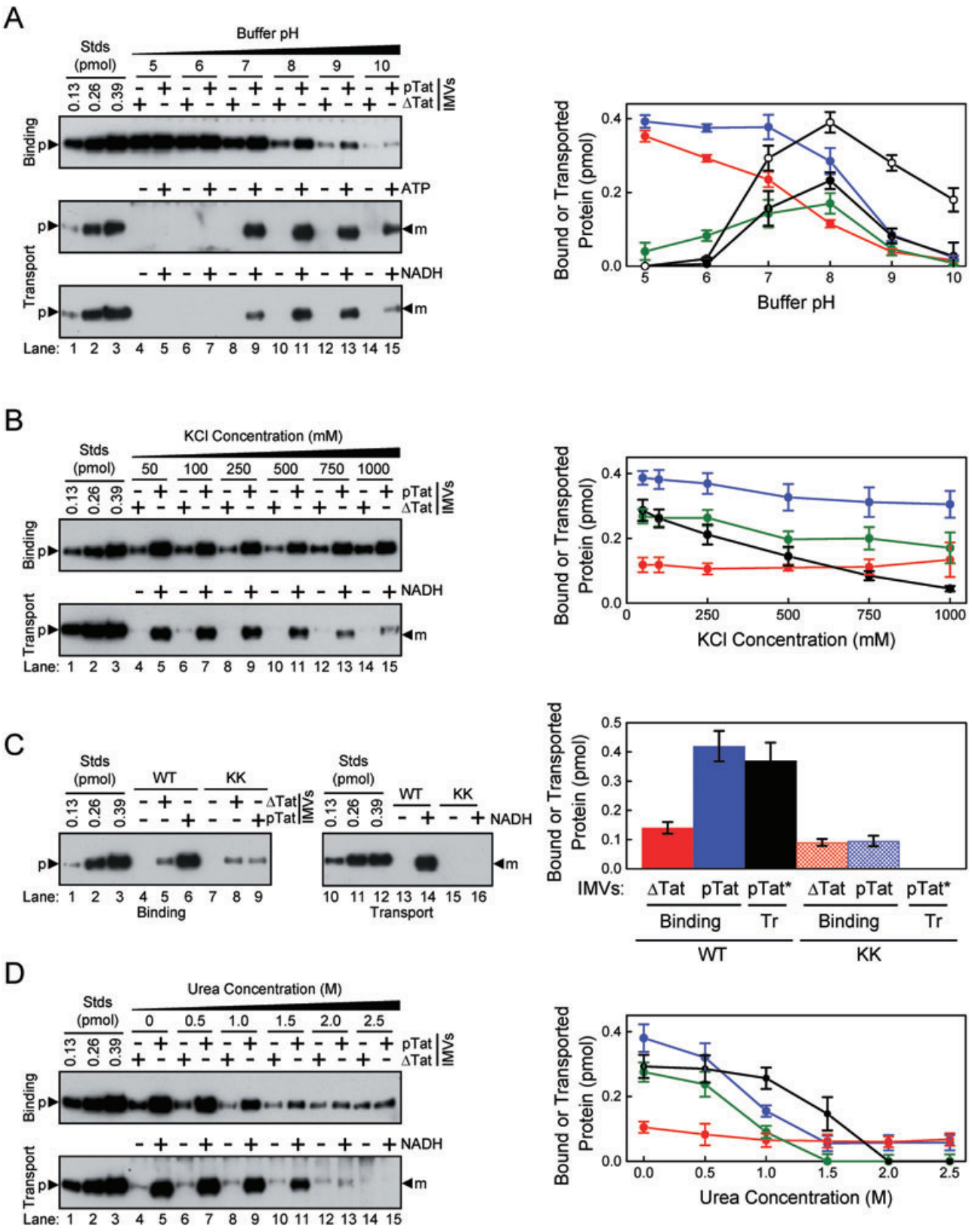

here. The precursor–lipid interactions were essentially unaffected by a range of KCl concentrations (0.05–1 M). In comparison, the amount of precursor bound to the Tat machinery decreased by ~35% over this KCl concentration range (Fig. 2B). Thus, both types of pre-SufI binding interactions are largely unaffected by salt concentration, suggesting that they are dominated by non-ionic interactions. In contrast, transport was largely blocked (by ~85%) by high KCl concentrations (Fig. 2B). One possibility is that ionic interactions at later stages of translocon assembly or downstream conformational changes are affected by high salt concentrations. Alternatively, PMF generation or maintenance could be affected. We did not pursue these issues further. However, we did test a mutant in which the double arginine motif in the signal peptide was mutated to KK (pre-SufI-KK). This mutant was shown previously to be transport incompetent (Stanley *et al*., 2000). As expected, pre-SufI-KK did not transport. Furthermore, pre-SufI-KK did not even bind to Tat translocons (Fig. 2C), consistent with previous reports demonstrating that precursor binding to the TatBC complex is inhibited by the KK mutation (Cline and Mori, 2001; Alami *et al*., 2003; Gérard and Cline, 2006). However, the lipid-binding activity of pre-SufI-KK was largely unaffected, consistent with membrane binding studies with bacterial and thylakoid precursor proteins (Brüser *et al*., 2003; Hou *et al*., 2006).

Addition of urea has been useful as a tool to investigate hydrophobic binding interactions. Urea concentrations up to 2.5 M had virtually no effect on the interactions of pre-SufI with the membrane lipid. In contrast, pre-SufI was completely dissociated from Tat translocons by 2 M urea. Not surprisingly, transport efficiency was also completely blocked by 2 M urea. However, transport efficiency was virtually unaffected by 1 M urea, whereas translocon binding activity was inhibited by ~75% (Fig. 2D). These data suggest that the pre-SufI–translocon binding interactions are weaker in the presence of 1 M urea than in its absence yet still strong enough to promote transport. In other words, binding still occurs and promotes transport, yet the binding affinity is insufficiently strong for the precursor protein to be recovered in a sedimentation assay. Urea causes solvation of hydrophobic groups, thus weakening the hydrophobic effect (Beck *et al*., 2007; Stumpe and Grubmüller, 2007; Hua *et al*., 2008; Stumpe and Grubmüller, 2008). Therefore, we speculate that urea interferes with translocon binding interactions by weakening the interaction between the h-domain of the signal peptide and a hydrophobic pocket on the Tat machinery.

Other precursor proteins

We next tested whether the membrane binding and transport characteristics observed for pre-SufI were unique or could be generalized. The first construct that we tested was spSufI-GFP, which consists of the signal peptide from pre-SufI attached to GFP. In earlier work, we showed that spSufI-GFP does not transport in *in vitro* assays, and does not even compete with pre-SufI for transport (Bageshwar and Musser, 2007). The latter result suggested that spSufI-GFP does not even bind to the Tat translocon. We directly tested this hypothesis here. We found that spSufI-GFP does not bind at all to IMVs, neither to the membrane lipids nor to the Tat translocon (Fig. 3A). These results demonstrate that the signal peptide is not the sole determinant of binding. The model construct spTorA-GFP, which contains the signal peptide from pre-TorA, is commonly used as a model cargo (Santini *et al*., 2001; Thomas *et al*., 2001; Barrett *et al*., 2003; DeLisa *et al*., 2004; Bageshwar and Musser, 2007). The translocon binding activity of spTorA-GFP saturates at ~4 pmol (Fig. 3A), similar to that observed for pre-SufI (Fig. 1C). These data therefore suggest a similar translocon binding affinity for TorA-GFP and pre-SufI. Next, the binding characteristics of spTorA-GFP were probed using urea and KCl (Fig. 3B). The results can be summarized as follows. Whereas 2 M urea did not affect the interaction of pre-SufI with the lipids, it inhibited the lipid binding interaction of spTorA-GFP by ~60%. The lipid binding interaction of spTorA-GFP was enhanced by 1 M KCl (by ~30%), whereas for pre-SufI it had essentially no effect. Urea and KCl acted synergistically on pre-SufI, causing almost complete dissociation from the Tat machinery and the membrane lipids. However, their effects on spTorA-GFP were largely the same as that observed with urea alone. Increasing the length of the linker between the spTorA-GFP signal peptide from four residues to 12 residues (yielding spTorA12-GFP) had essentially no effect on lipid or translocon binding interactions. These data indicate that different Tat precursors have different affinities towards the membrane lipid and the Tat translocons, which are determined by different ionic and hydrophobic interactions. Importantly, however, both binding modes are still apparent and readily distinguishable. Thylakoid Tat precursors are also completely dissociated from the membrane surface by a combination of urea and KCl, but urea or KCl alone have different effects on different precursors (Gérard and Cline, 2006; 2007), as we observed here.

We next compared the transport efficiencies of spTorA-GFP and spTorA12-GFP under single- and multiple-turnover conditions (Fig. 3C). spTorA-GFP behaved similar to pre-SufI in that ATP caused an increase in transport efficiency (~2-fold), compared with that observed with NADH. Further, the amount of spTorA-GFP transported with NADH (0.4 $\pm$ 0.1 pmol) was comparable with that which bound to the Tat machinery (0.5 $\pm$ 0.1 pmol). However, when IMVs were energized with ATP, a significantly higher transport yield was

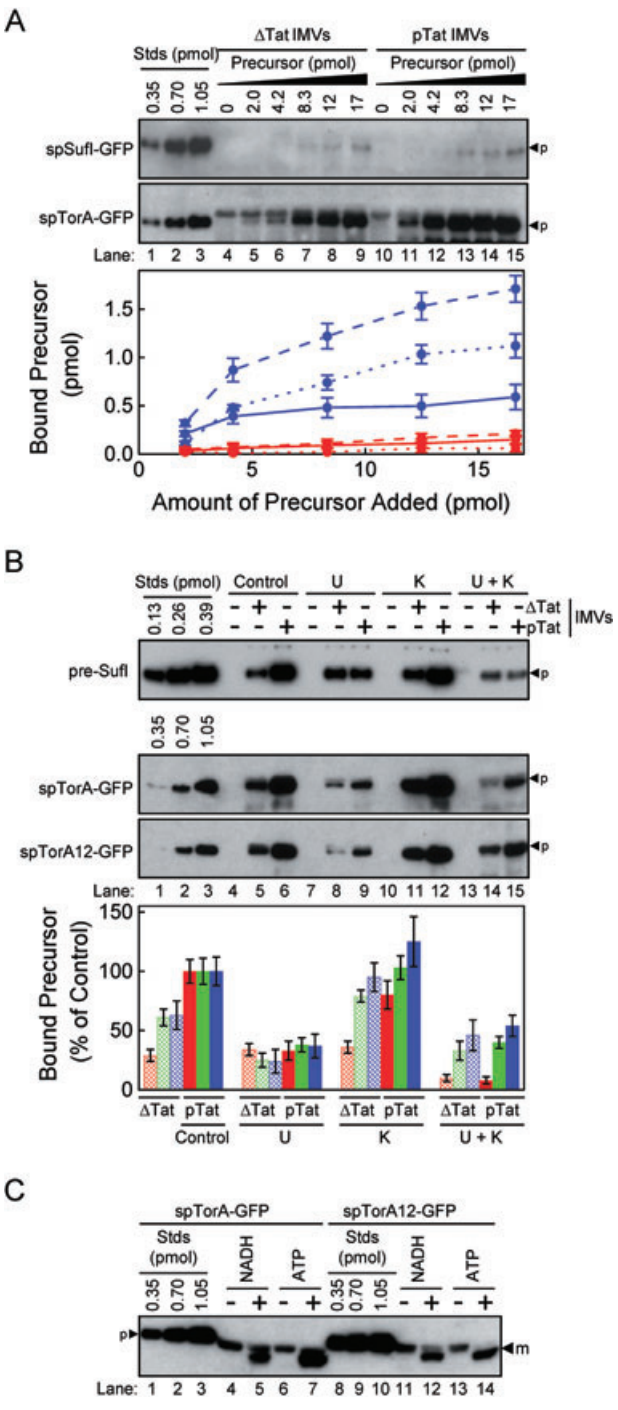

Fig. 3. Effect of chemical agents on the membrane binding and transport efficiency of GFP precursors. The gels in this figure are anti-SufI (B, top) or anti-GFP (all others) immunoblots.
A. Concentration dependence of the binding efficiency of spTorA-GFP and spSufI-GFP. The data were quantified as in Fig. 1C: (dashed) precursor bound to pTat IMVs, (dotted) lipid-bound precursor, (solid) translocon-bound precursor, (blue) spTorA-GFP, and (red) spSufI-GFP ($n = 3$). The upper band on the anti-GFP immunoblot results from immuno-crossreactivity to a non-GFP protein and was only occasionally observed.
B. Effect of 2 M urea (U), 1 M KCl (K) and 2 M urea + 1 M KCl (U + K) on the membrane binding efficiency of pre-SufI (red), spTorA-GFP (green) and spTorA12-GFP (blue). The plot shows averaged data ($n = 3$) for ΔTat (hatched) and pTat (solid) IMVs. The precursor bound to pTat IMVs is considered the control (100%).
C. Effect of the magnitude of the PMF on the transport efficiency of spTorA-GFP and spTorA12-GFP. In B and C, 8.3 pmol of spTorA-GFP and spTorA12-GFP was added to the reactions; in B, 3.1 pmol of pre-SufI was added.

observed (0.8 ± 0.2 pmol) (Fig. 3C). These data imply that additional spTorA-GFP must bind to Tat translocons during ATP driven transport. A similar result was observed for pre-SufI (Fig. 2A). Interestingly, spTorA12-GFP behaved differently than spTorA-GFP under ATP-driven transport conditions in that there was no enhancement in transport efficiency compared with NADH-driven transport. We do not have an explanation for this result.

Importance of hydrophobicity at position 17 of the pre-SufI signal peptide

In order to develop a simpler, non-Western blot-based binding and transport assay, and to better study the kinetics of Tat transport, we sought a fluorescent precursor that was efficiently transported. As spTorA-GFP was transported less efficiently than pre-SufI, we sought a fluorescent version of pre-SufI, e.g. one that could be prepared by modification of cysteine residues through maleimide chemistry. Wild-type pre-SufI contains two cysteines, C17 and C295 (Fig. 4A). As labelling experiments indicated that the C295 residue of pre-SufI was not highly reactive towards maleimides, a cysteine was added at the C-terminus to provide an additional labelling site, generating pre-SufI-CCC. The pre-SufI and pre-SufI-CCC proteins exhibited similar membrane binding and transport activities (Fig. 4B). Faced with the task of removing the cysteine in the signal peptide, we constructed the C17S mutant. The transport efficiency of the C17S mutant was ~85% less than that of wild-type pre-SufI. Therefore, we randomly mutageneized the C17S mutant using degenerate primers. Plasmids from 41 colonies were sequenced, yielding 10 new unique mutants. The C17W mutation was generated with specific primers. The membrane binding and transport properties of pre-SufI with 13 different residues at position 17 are summarized in Fig. 4C (raw data in Fig. S2). Every C17 mutant tested displayed a substantially reduced capacity to bind to the membrane lipids. All but three mutants (C17M, C17W and C17I) exhibited reduced translocon binding activity. All but one mutant (C17I) displayed reduced transport activity.

One possible explanation of the C17 mutant data is that the h-domain of the signal peptide strongly influences the partitioning of the pre-SufI signal peptide into the hydrophobic interior of the lipid bilayer and into a hydrophobic groove in the Tat translocon (signal peptide binding site). Such a partitioning is expected to generally follow the

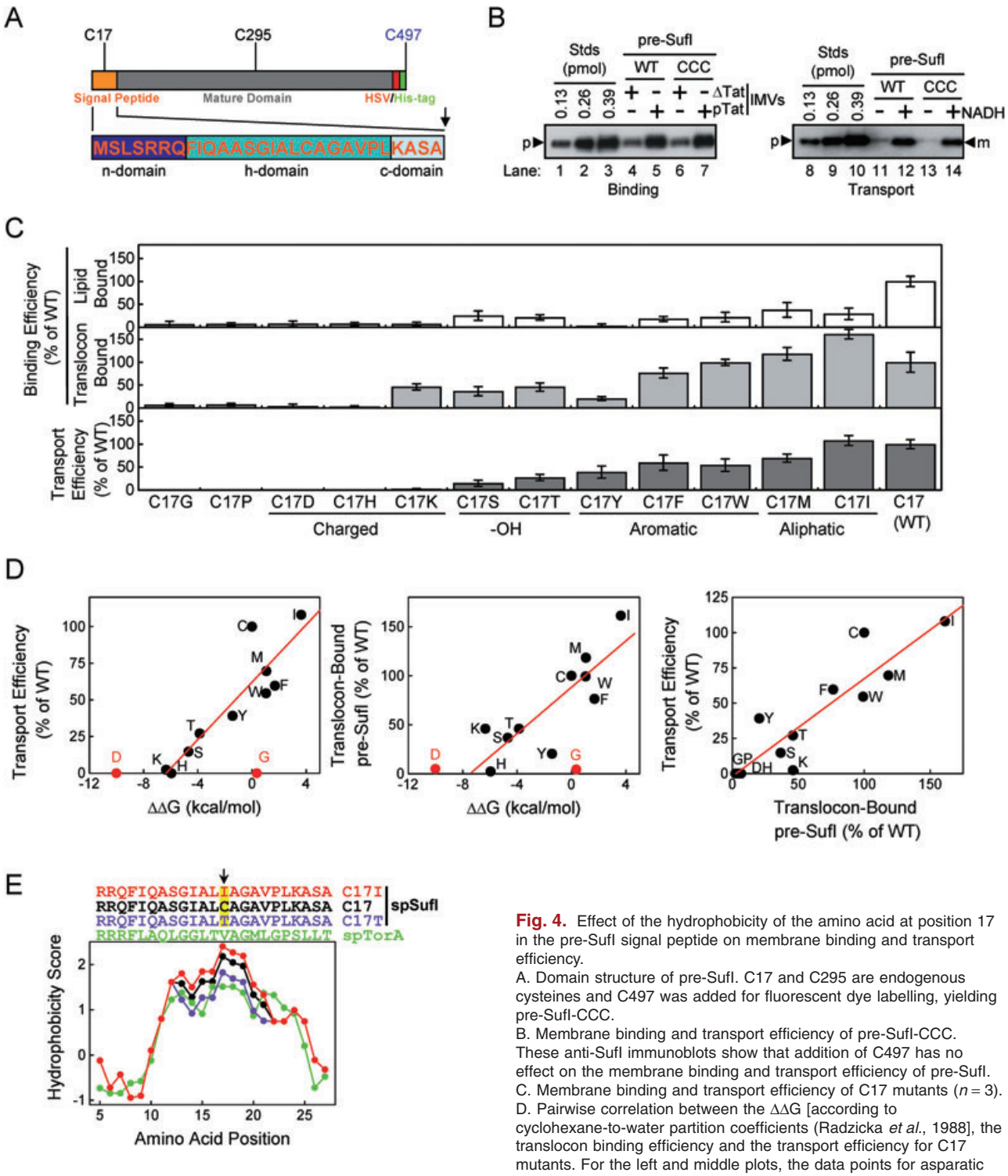

Fig. 4. Effect of the hydrophobicity of the amino acid at position 17 in the pre-SufI signal peptide on membrane binding and transport efficiency.
A. Domain structure of pre-SufI. C17 and C295 are endogenous cysteines and C497 was added for fluorescent dye labelling, yielding pre-SufI-CCC.
B. Membrane binding and transport efficiency of pre-SufI-CCC. These anti-SufI immunoblots show that addition of C497 has no effect on the membrane binding and transport efficiency of pre-SufI.
C. Membrane binding and transport efficiency of C17 mutants ($n = 3$).
D. Pairwise correlation between the ΔΔG [according to cyclohexane-to-water partition coefficients (Radzicka *et al.*, 1988], the translocon binding efficiency and the transport efficiency for C17 mutants. For the left and middle plots, the data points for asparatic acid (D) and glycine (G) were not included in the best-fit line determination because they appear to be outliers. Once the transport efficiency reaches zero, a more negative ΔΔG is expected to have no effect, which explains the D point.
E. Kyte and Doolittle (Kyte and Doolittle, 1982) hydropathy plot for the signal peptides of pre-SufI (black), pre-SufI-ICC (red), pre-SufI-TCC (violet) and pre-TorA (green) using a scanning window of nine residues.

predictions of amino acid hydrophobicity according to one of the numerous proposed free energy scales. The transport efficiency of the various C17 mutants displayed a reasonably linear correlation with the free energy change of the mutation, according to cyclohexane-to-water partition coefficients (Fig. 4D, left panel). Strongly hydrophilic, charged substitutions (C17D, C17H and C17K mutations) led to complete inhibition of transport. Such substitutions are expected to adversely affect hydrophobic interactions. Aliphatic substitutions (C17M and C17I) retained good transport activity, consistent with being conservative substitutions. Translocon binding activity was moderately correlated with the cyclohexane-to-water hydrophobicity scale (Fig. 4D, middle panel). The transport activity of pre-SufI was moderately correlated with its translocon binding activity (Fig. 4D, right panel). Variations from linearity likely arise from steric issues. The moderately lower hydrophobicity of the central h-domain of the TorA signal peptide compared with that of pre-SufI (Fig. 4E) may explain, at least in part, the lower transport efficiency of spTorA-GFP (Bageshwar and Musser, 2007). Although highly hydrophobic h-domains can convert Tat signal peptides into Sec targeting domains (Cristóbal *et al.*, 1999), the slight increase in h-domain hydrophobicity of the C17I pre-SufI mutant is apparently insufficient to inhibit Tat targeting.

The C17I mutant

Based on the data discussed in the previous section, the C17I mutant appeared to be the most useful for an efficient fluorescence-based transport assay: it is the most selective for translocon interactions over lipid interactions (~10:1), and it is the most efficiently transported (110 ± 9% as compared with pre-SufI-CCC). Therefore, we further examined the properties of this mutant. From the membrane binding activity of pre-SufI-ICC measured over a range of concentrations (Fig. 5A), it is clear that the lipid binding activity of pre-SufI-ICC is very low. One potential complication that could arise with a precursor protein that binds to both lipids and translocons is that the amount bound to each is expected to depend on the lipid to translocon ratio. As shown in Fig. S3, this complicating issue disappears for the C17I mutant. We next examined the translocation activity of the C17I mutant over a range of concentrations. The amount of translocated precursor was well correlated with the amount of translocon-bound precursor (Fig. 5B), in agreement with earlier results (Figs 1C and 4D).

Transport of fluorescent pre-SufI

The endogenous cysteine within the mature domain of pre-SufI-ICC was replaced with alanine (C295A), yielding a pre-SufI mutant (pre-SufI-IAC) with a single cysteine at the C-terminus, immediately downstream of the 6xHis-tag. The transport efficiency of pre-SufI-IAC was indistinguishable from that of pre-SufI-ICC (Fig. 6A). The cysteine of pre-SufI-IAC was labelled with Atto565 maleimide, yielding pre-SufI-IAC^{atto}. Unlabelled and Atto565-labelled pre-SufI-IAC showed indistinguishable transport efficiencies and binding affinities towards membrane lipids and Tat translocons (Fig. 6B). The transport kinetics of fluorescent and non-fluorescent pre-SufI-IAC, as monitored by Western blotting and direct in-gel fluorescence imaging, were indistinguishable (Fig. 6C). Thus, pre-SufI-IAC^{atto} is an efficiently transported fluorescent Tat substrate that behaves identically to the unlabelled protein.

Avidin blocks translocation of biotinylated pre-SufI

A major question that arises from the data presented thus far is whether lipid-bound precursors reside in a dead-end state and must dissociate from the membrane before they can possibly be translocated, or whether they can proceed from the lipid-bound state directly to the translocon-bound state for transport. The latter scenario was first suggested for the thylakoid Tat machinery based on the behaviour of a transport incompetent precursor (Musser and Theg, 2000). When avidin was added to an import reaction containing biotinylated and unbiotinylated precursor, the biotinylated precursor was not translocated yet it still bound to thylakoid membranes and competitively inhibited transport of the unbiotinylated precursor. One explanation is that the lipid-bound state of the precursor protein is an intermediate in the transport process. If so, lipid-bound avidin–precursor complexes might be sufficient to inhibit transport of unbiotinylated precursor. What was unclear in these experiments, however, was whether the avidin–precursor complex could bind to the Tat machinery. We sought here to test this hypothesis.

The original basic principle behind the experiments with biotinylated precursor protein was to generate a translocation intermediate, i.e. a precursor undergoing transport stuck within the translocon. Addition of avidin to a biotinylated protein results in a very strong, non-covalent interaction between the biotin moiety and the avidin. The resultant precursor–avidin complex is much different in size and shape from the precursor alone. Such characteristics might cause the precursor to become stuck at an intermediate state of transport. Biotinylated pre-SufI-IAC (pre-SufI-IAC^{biotin}) was generated by reaction of pre-SufI-IAC with biotin maleimide. Avidin blocked transport of pre-SufI-IAC^{biotin} when the transport reaction was initiated with NADH, unless free biotin was premixed with the avidin (Fig. 7A). These data support the hypothesis that avidin blocks transport by binding to the biotin moiety on the precursor protein. The pre-SufI-IAC^{biotin}–avidin

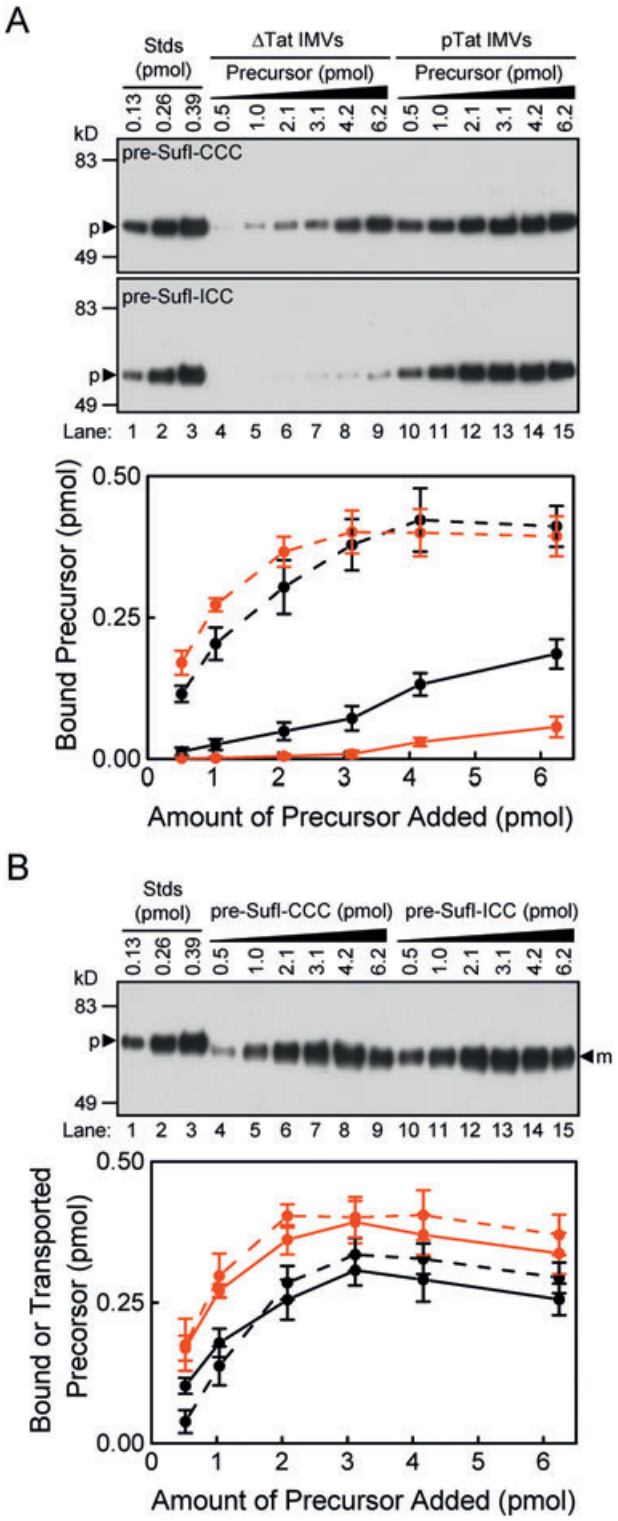

Fig. 5. Membrane binding and transport efficiency of pre-SufI-ICC. All gels in this figure are anti-SufI immunoblots.
A. Concentration dependence of membrane binding efficiency. The amount of pre-SufI-CCC (black) and pre-SufI-ICC (red) bound to ΔTat (solid) and pTat IMVs (dashed) was quantified ($n = 3$).
B. Correlation between transport efficiency and the amount of translocon-bound precursor. The gel shows the concentration-dependent transport efficiency of pre-SufI-CCC and pre-SufI-ICC using 4 mM NADH. The plot shows the amount of transported pre-SufI-CCC (black) and pre-SufI-ICC (red) from three independent experiments (solid lines). The amount of translocon-bound protein was calculated from the data in A as described in Fig. 1C (dashed lines).

complex competitively inhibited the transport of unbiotinylated pre-SufI-IAC in the presence and absence of avidin (Fig. 7B). These results (Fig. 7A and B) are qualitatively identical to those reported earlier for the thylakoid Tat complex (Musser and Theg, 2000). Interestingly, the pre-SufI-IAC^{biotin}–avidin complex binds almost as strongly to the Tat machinery as pre-SufI-IAC^{biotin} alone, and it does not matter whether the precursor is incubated first with IMVs or first with avidin (Fig. 7C). Thus, the avidin moiety does not prevent pre-SufI-IAC^{biotin} from interacting with the Tat machinery. These data therefore indicate that avidin blocks transport of pre-SufI-IAC^{biotin} at some step after the initial translocon binding step. Somewhat surprisingly, avidin enhanced the ability of pre-SufI-IAC^{biotin} to bind to the membrane lipids (Fig. 7C). This result can be explained by a non-specific interaction of avidin with the membrane lipids.

To probe the strength of the interaction between pre-SufI and the Tat translocon, a near saturating concentration (90 nM, 3.1 pmol) of both pre-SufI-IAC^{biotin} and pre-SufI-IAC^{atto} were incubated with IMVs in the presence of avidin. However, we varied the order of addition of the two precursor proteins. If the translocon-bound form of the precursor was a strong interaction, implying a slow off-rate, pre-incubation of IMVs with pre-SufI-IAC^{atto} should lead to translocon-bound precursor that can be chased into the lumen of the IMVs after NADH addition even in the presence of precursor–avidin complexes. However, this was not seen (Fig. 7D, lane 9). Instead, the transport of fluorescent pre-SufI was strongly inhibited by precursor–avidin complexes, whether these complexes were added before, after, or at the same time as the fluorescent pre-SufI (Fig. 7D, lanes 7–9). These data suggest that a translocon-bound precursor molecule can relatively rapidly exchange with another precursor molecule, irrespective of whether either molecule is attached to an avidin molecule through a biotin linkage. Note that the precursor–avidin complexes are more inhibitory at a higher total precursor concentration (compare Fig. 7B and D), for unknown reasons.

Interconversion between lipid- and translocon-bound forms of pre-SufI

We next sought to more directly investigate whether the lipid- and translocon-bound forms of pre-SufI could

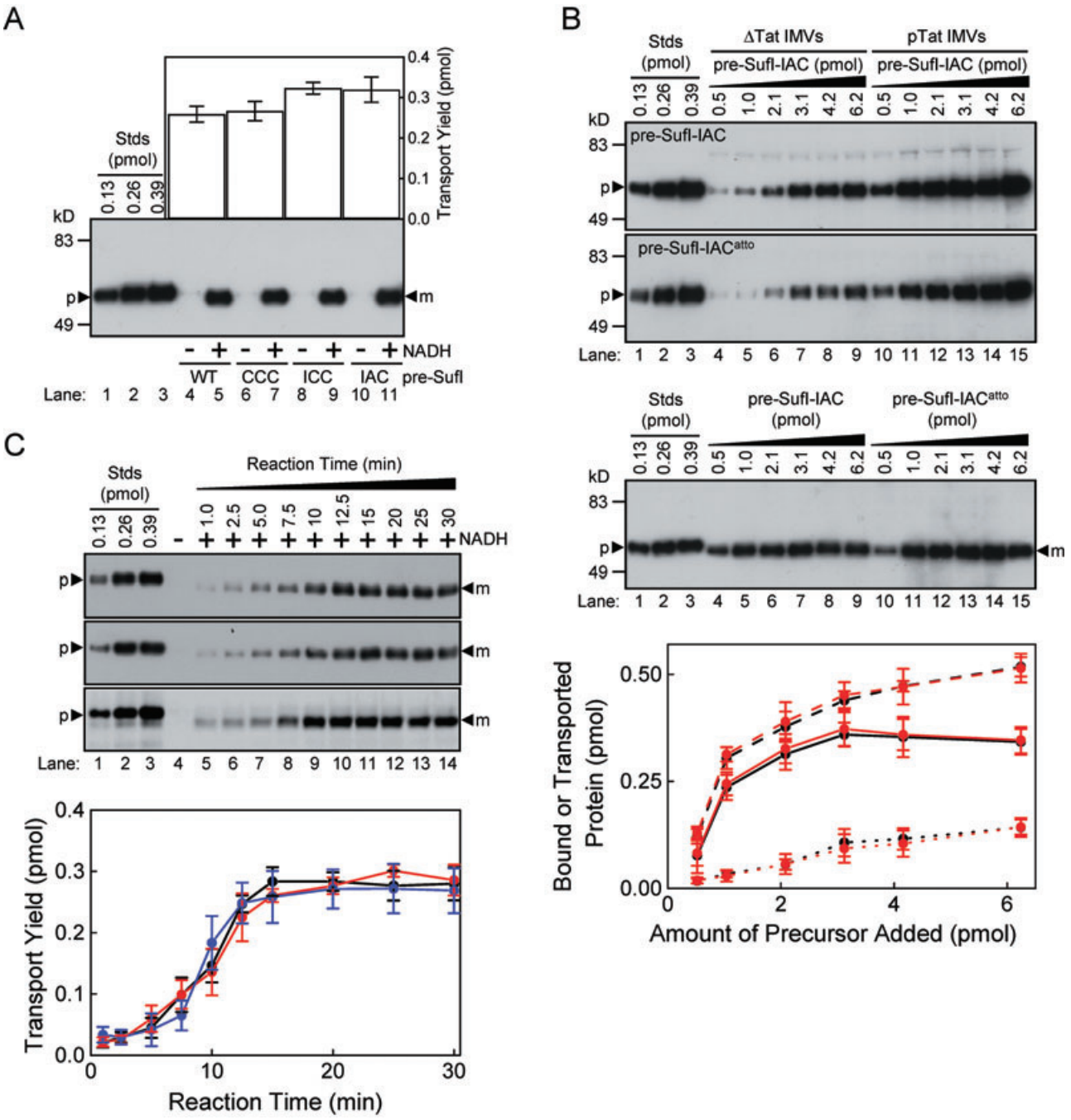

Fig. 6. Transport kinetics of Atto565-labelled pre-SufI.
A. Transport of pre-SufI, pre-SufI-CCC, pre-SufI-ICC and pre-SufI-IAC ($n = 3$). 3.1 pmol (90 nM) precursor protein was added to each reaction.
B. Membrane binding and transport efficiency of pre-SufI-IAC^{atto}. The membrane binding efficiency of unlabelled (top) and Atto565-labelled (middle) pre-SufI-IAC to ΔTat and pTat IMVs was determined for various precursor concentrations. The transport yield (bottom) of both of these precursors was determined with 4 mM NADH and pTat* IMVs. The plot shows the quantified results: (black) pre-SufI-IAC, (red) pre-SufI-IAC^{atto}, (dotted) lipid-bound precursor, (dashed) lipid + translocon-bound precursor and (solid) transported precursor ($n = 3$). All gels in A and B are anti-SufI immunoblots.
C. Transport kinetics of pre-SufI-IAC^{atto}. The top and middle gels are anti-SufI immunoblots of pre-SufI-IAC (black) and pre-SufI-IAC^{atto} (red) respectively. In the bottom gel, the Atto565-labelled protein was detected by fluorescence emission (blue) ($n = 3$).

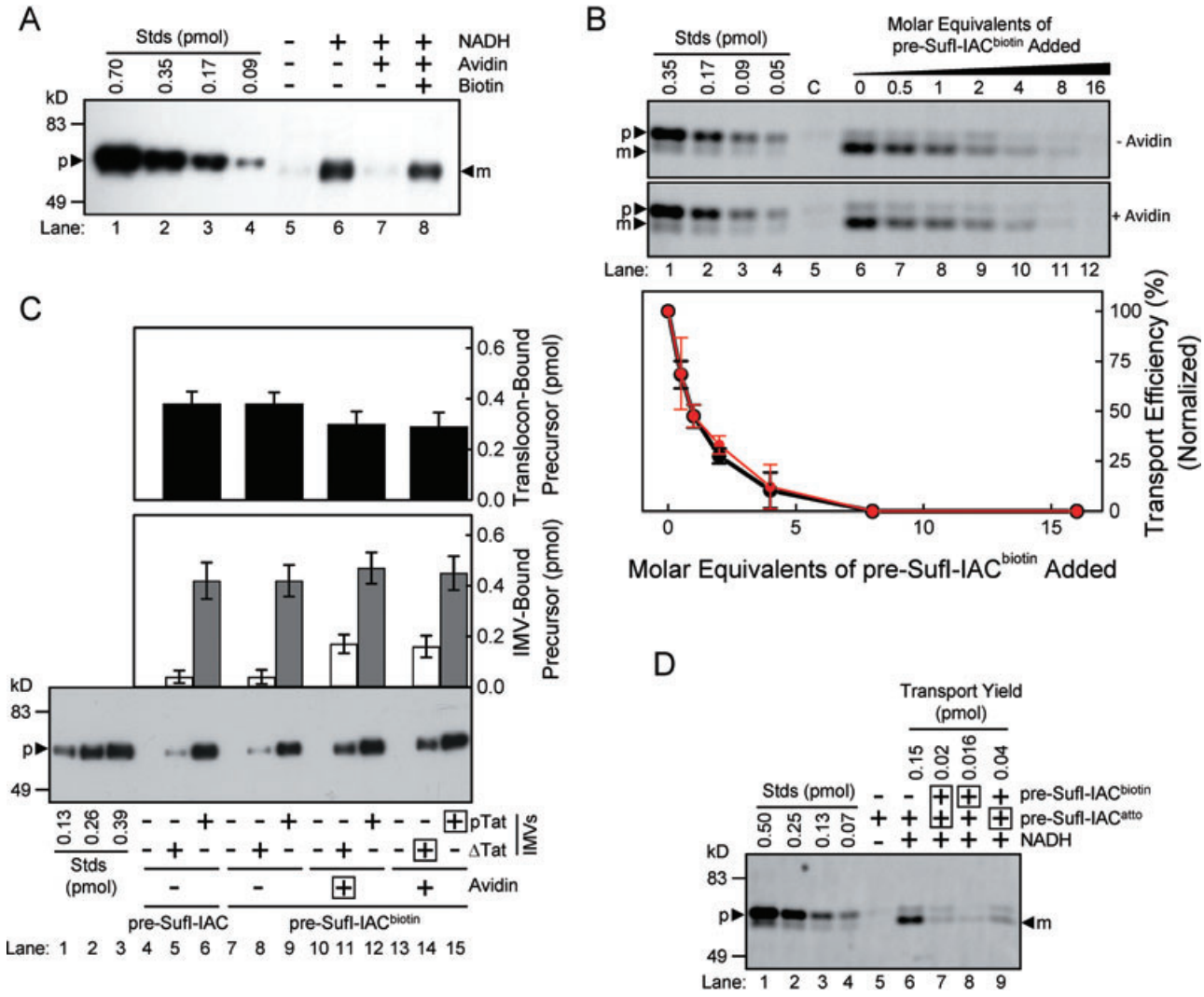

Fig. 7. Properties of the pre-SufI-IAC^{biotin}/avidin complex.
A. Effect of avidin on the transport of pre-SufI-IAC^{biotin}. Proteins were detected by Western blotting using avidin-HRP. When present, biotin (16 μM) was in large excess over neutravidin (1.6 μM), and neutravidin was in large excess over the precursor protein (40 nM, 1.4 pmol). Thus, the binding interactions were saturated. [IMV] = 5 (A_{280}).
B. Competition between pre-SufI-IAC^{biotin} and pre-SufI-IAC^{atto} in the presence of avidin. The transport efficiency of pre-SufI-IAC^{atto} (40 nM, 1.4 pmol) was determined in the absence (black) and presence (red) of 25 μM neutravidin and the indicated molar equivalents of pre-SufI-IAC^{biotin} ($n = 3$). Gels were visualized by the Atto565 fluorescence emission. [NADH] = 4 mM; [IMV] = 5 (A_{280}).
C. Membrane binding efficiency of pre-SufI-IAC^{biotin} in the presence of avidin. This anti-SufI immunoblot shows the binding efficiency of pre-SufI-IAC and pre-SufI-IAC^{biotin} to ΔTat and pTat IMVs in the presence and absence of 25 μM neutravidin, as indicated. In lanes 10–15, the boxes indicate which reagent was added first. In lanes 10–12, neutravidin was pre-incubated with pre-SufI-IAC^{biotin} for 10 min prior to addition of IMVs ($A_{280} = 2$). In lanes 13–15, IMVs were pre-incubated with pre-SufI-IAC^{biotin} for 10 min prior to addition of neutravidin. The lower plot corresponds to integrated values from the lanes below in the gel (averaged over three identical experiments). The upper plot corresponds to the amount of translocon-bound precursor, calculated for each set of experiments by subtracting the ΔTat IMV values from the pTat IMV values.
D. Effect of precursor addition order on the transport efficiency of pre-SufI-IAC^{atto}. For lanes 5–9, the reactions contained pre-SufI-IAC^{atto}, 25 μM neutravidin, and pTat* IMVs ($A_{280} = 5$). For lanes 7–9, the reactions contained pre-SufI-IAC^{biotin}. The boxes indicate which precursor (90 nM, 3.1 pmol each) was added first to the reaction solution. In lane 7, both precursors were added simultaneously, and 4 mM NADH was added 5 min later. In lane 8, pre-SufI-IAC^{biotin} was added 5 min prior to the simultaneous addition of pre-SufI-IAC^{atto} and NADH. Lane 9 was obtained similarly to lane 8, but the precursors were reversed. This gel was visualized by the Atto565 fluorescence emission.

interconvert. In multiple ATP-driven transport experiments (Figs 2A and 3C), the transport yield was larger than the amount of precursor protein bound to Tat translocons. This extra protein had to come from the soluble (aqueous) phase, from the pool of lipid-bound precursor protein, or from both precursor reservoirs. To eliminate the soluble precursor protein, pre-SufI was pre-incubated with pTat* IMVs and the mixture was then centrifuged (Fig. 8). The recovered IMVs contained precursor protein strongly bound to the membrane because essentially no pre-SufI

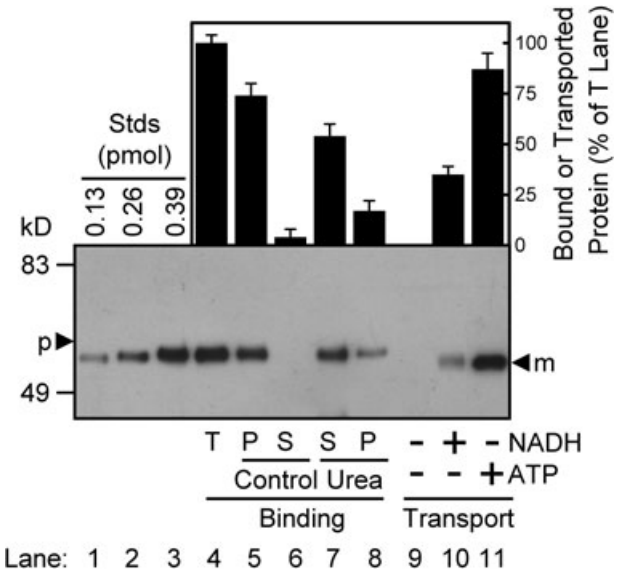

Fig. 8. Transport of lipid-bound precursor. Pre-SufI (90 nM) was incubated with pTat* IMVs for 10 min at 37°C. IMVs were recovered by centrifugation through a 0.7 M sucrose cushion to remove the unbound precursor protein (*Experimental procedures*). Lane 4 of this anti-SufI immunoblot shows the total (T) amount of pre-SufI bound to the IMVs. To probe the reversibility of the membrane binding reaction, IMVs with bound pre-SufI were incubated at 37°C for 10 min and re-isolated by centrifugation. Most of the pre-SufI was recovered with IMVs in the pellet (P) fraction (lanes 5–6). In contrast, addition of 2 M urea resulted in the release of a significant fraction of the membrane-bound pre-SufI into the supernatant (S) fraction (lanes 7–8). In the presence of ATP, more pre-SufI was transported than was released from the membrane by urea (compare lanes 11 and 7), indicating that some of the lipid-bound precursor must have transported under these conditions. For this figure, pTat* IMVs were used for both the membrane binding experiments and the transport experiments ($n = 3$). [IMVs] = 2 (A_{280}) for each lane.

was recovered in the supernatant upon re-centrifugation (Fig. 8, lane 6). Urea dissociated ~3/4 of the membrane-bound pre-SufI (Fig. 8, compare lanes 7 and 5), consistent with the hypothesis that the majority of the precursor was bound to Tat translocons (compare with Fig. 3B). When NADH was added, ~1/3 of the initially recovered precursor was transported (Fig. 8, compare lanes 10 and 4). However, when ATP was added almost all of the initially recovered precursor was transported (Fig. 8, compare lanes 11 and 4). As significantly more precursor was transported upon ATP addition than was initially bound to translocon components (Fig. 8, compare lanes 11 and 7), additional precursor must have been recruited to the translocons during the incubation period. As there was essentially no soluble precursor present in the reaction (Fig. 8, lane 6), the additional precursor must have come from the lipid-bound precursor reservoir. Thus, these data suggest that the lipid- and translocon-bound forms of pre-SufI can directly interconvert, i.e. that the lipid-bound form of the precursor can laterally diffuse to the translocation machinery, bind to it, and undergo transport.

Discussion

The major finding of this study is two distinct membrane binding modes for bacterial Tat precursor proteins. The first of these binding interactions is the expected binding interaction with the TatABC proteins. The second membrane binding interaction is not mediated by any of the Tat proteins, because this interaction was detectable in a ΔTatABCDE strain (Fig. 1C). Due to the known affinity of Tat precursors and signal peptides for pure lipid membranes (Musser and Theg, 2000; Hou *et al.*, 2006; Shanmugham *et al.*, 2006), the retention of the non-Tat binding interaction in trypsinized membranes (Fig. 1D), and the dramatic effects on binding of single site mutations in the signal peptide (Fig. 4C), we ascribe the second binding mode to a direct interaction between the membrane lipids and the signal peptide. Whether this interaction is an adsorption to the membrane surface, or a partial or full penetration of the membrane bilayer by the signal peptide requires further investigation. Although it has been suggested that a membrane ATPase promotes the integration of the signal sequence into the membrane bilayer (Brüser *et al.*, 2003), we find that the lipid binding interaction is ATP-independent and occurs after shaving the membrane with protease (Fig. 1D), suggesting that an ATPase is not involved. The lipid-bound precursor can be chased into the IMV lumen in the presence of ATP (Fig. 8), indicating that the lipid-bound precursor remains translocation competent. We consider it unlikely that an ATPase is involved in the transfer of the precursor from the lipid to the translocon, and surmise that this ATP effect results simply from a longer-lived, higher magnitude PMF (Bageshwar and Musser, 2007). The lipid-bound precursor state we identified corresponds well with the Tm-1 state identified in thylakoid binding studies (Hou *et al.*, 2006). A model of the Tat transport cycle as discussed in the Introduction and consistent with the data presented here is shown in Fig. 9.

The two distinct membrane binding modes for Tat precursor proteins are distinguishable by their differential susceptibility to urea and KCl. As urea reduces the binding affinity of precursors for Tat translocons, the translocon binding interactions appear to be mediated, at least in part, by hydrophobic interactions. For the bacterial Tat precursors examined, the data are consistent with the hypothesis that the h-domains of the signal peptides bind in a hydrophobic groove of the TatBC complex (McDevitt *et al.*, 2006; Holzapfel *et al.*, 2007). Mutation of the double arginine motif to KK led to the complete loss of translocon binding (Fig. 2C). As this is a conservative mutation, the translocon binding site is sufficiently selective that it can

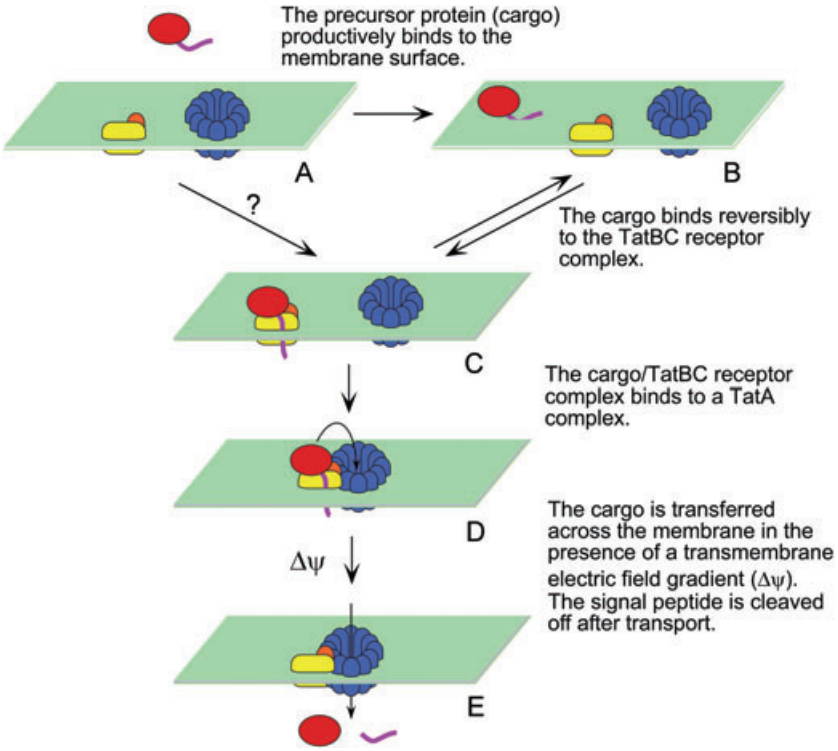

Fig. 9. Model of *E. coli* Tat transport. TatB (orange) and TatC (yellow) form a receptor complex, and TatA (blue) forms ring-like oligomers in resting membranes (A). The precursor protein (red) binds to the membrane surface (B) in addition to its binding site on the TatBC complex (C). The cargo/TatBC complex associates with an oligomerized TatA complex (D). Cargo is transported across the membrane in the presence of a transmembrane electric field gradient (Δψ). Signal peptide (purple) cleavage occurs after transport of the precursor protein (E). We reported earlier that there are two ψ-dependent steps (Bageshwar and Musser, 2007). The first Δψ-dependent step can occur in the absence of precursor protein (not shown). The second Δψ-dependent step occurs after the precursor protein binds to the membrane, suggested here as the D → E step. For clarity, the likely possibility that the TatBC complexes form higher-order oligomers (Tarry *et al.*, 2009) is not shown. The fate of the signal peptide after transport is not known.

distinguish between lysine and arginine, perhaps by recognizing the guanidinium group on the latter. However, the charge of the side-chain does not dominate the binding affinity (although it may certainly contribute), because high salt concentrations have little effect on the translocon binding interaction (Fig. 3B). Interestingly, both KK and AA versions of pre-SufI co-immunoprecipitated with the TatBC complex when expressed under *in vivo* conditions (McDevitt *et al.*, 2006). In light of our data, these results can be explained by binding of the pre-SufI mutants to lipid within the detergent micelles containing the purified TatBC complexes. The strong binding of the translocation incompetent KK mutant of the reduced TorA-PhoA protein to Tat-containing IMVs (Panahandeh *et al.*, 2008) can be explained, at least in part, by binding to the membrane lipids.

The finding that the bacterial Tat precursor pre-SufI remains strongly bound to the IMV surface once bound (Fig. 8) agrees with previous results on the thylakoid Tat system, which also indicated strong membrane binding (Musser and Theg, 2000; Hou *et al.*, 2006). However, we found here that the lipid- and translocon-bound forms of the precursor appear readily exchangeable (Fig. 7D). This conclusion may help explain why it has been so difficult to generate a translocation intermediate for the Tat machinery – the precursor simply does not bind tightly to the translocon. The tight membrane binding interaction must therefore be provided by the non-Tat binding interaction. Our previous result that a precursor could compete for transport despite being added ~5 min after initiation of transport with NADH (Bageshwar and Musser, 2007) is difficult to comprehend in the context of a strong, stable interaction of the signal sequence with the Tat translocon. However, this result is much easier to comprehend now, knowing that the membrane-bound forms of the precursor rapidly interconvert. Precursor proteins could bind and dissociate from the translocon on a relatively rapid timescale, and a translocon interaction may only occasionally lead to cargo transport.

An important question is whether the lipid-bound form of the precursor protein is a necessary intermediate within the transport cycle. Here we have showed that this state exists under *in vitro* conditions and that it represents a pool of transport competent precursor protein. *In vivo*, one role of precursor-specific chaperone proteins, such as DmsD, NapD, HybE and TorD (Oresnik *et al.*, 2001; Dubini and Sargent, 2003; Jack *et al.*, 2004; Maillard *et al.*, 2007) may be to minimize lipid binding reactions. It is unknown how deeply the signal sequence penetrates into the lipid bilayer. If the signal sequence binds to the translocon from a position deeply embedded within the lipid bilayer, it is difficult to envision how a signal sequence could also find the translocon directly from the aqueous phase. Thus, if the signal sequence embeds deeply within the lipid bilayer, the lipid-bound state would likely be a necessary intermediate for transport. On the other hand, the signal sequence may not penetrate deeply within the lipid bilayer and may have easy access

to the translocon binding site from the cytoplasm. However, the conclusion that the lipid- and translocon-bound forms of the precursor easily interconvert suggests that the lipid-bound state will be accessed during the normal transport process even if the soluble precursor binds directly to the translocon. Future work is needed to address these important issues. However, it is clear at this juncture that the lipid-bound form of Tat precursor proteins are important functional intermediates that should be acknowledged in models of the transport cycle.

Experimental procedures

Bacterial strains, plasmids and growth conditions

Escherichia coli strains MC4100, MC4100ΔTatABCDE, JM109 and BL21(λDE3) have been described earlier (Casadaban and Cohen, 1979; Yanisch-Perron *et al.*, 1985; Studier *et al.*, 1990; Wexler *et al.*, 2000). Overexpression cultures were grown in Luria–Bertani medium at 37°C supplemented with the appropriate antibiotics (Sambrook and Russell, 2001). Plasmids pET-SufI, pSufI-GFP and pTorA-GFP have been described earlier (Yahr and Wickner, 2001; Bageshwar and Musser, 2007). The protein constructs used here and the primers used to generate the necessary expression plasmids are provided in Tables S1 and S2. Plasmid pTorA12-GFP, which encodes 12 amino acid residues of the mature TorA protein between the TorA signal peptide and the GFP domain, was generated by inverse PCR using *Pfu* Turbo DNA polymerase (Stratagene), TorA12-F and TorA12-R as the primers, and pTorA-GFP as the template. All single amino acid changes were generated by QuikChange site-directed mutagenesis (Stratagene). Plasmid pSufI-CCC was constructed using primers 3′-Cys-F and 3′-Cys-R and the pET-SufI template. This plasmid encodes for pre-SufI-CCC, which contains an additional cysteine at the C-terminus of pre-SufI. Plasmid pSufI-SCC, which was generated using primers SufIC17S-F and SufIC17S-R and the pSufI-CCC template, encodes for pre-SufI-SCC, which has a C17S mutation in the signal peptide of pre-SufI. Position C17 in pre-SufI was randomly mutagenized by randomizing the codon (equal base probability at each position) using primers SufIC17N-F and SufIC17N-R and the pSufI-SCC template. A total of 41 clones were sequenced to obtain 10 mutants. The resultant plasmids and encoded proteins are designated pSufI-XCC and pre-SufI-XCC respectively, where the identity of the C17 mutation in the pre-SufI signal peptide is identified by the X. Plasmid pSufI-WCC was generated using primers SufIC17W-F and SufIC17W-R and the pSufI-SCC template. Plasmid pSufI-IAC, which encodes the C295A mutation in the mature domain of SufI, was generated using primers SufIC295A-F and SufIC295A-R and the pSufI-ICC template. Plasmid pSufI-KK-CCC, which encodes KK instead of the double-arginine motif, was generated using primers SufI-KK-F and SufI-KK-R (both primers are flanked by NdeI restriction endonuclease sites) and the pSufI-CCC template by inverse PCR using *Pfu* Turbo DNA polymerase. The PCR product was cleaved with NdeI and self-ligated to generate pSufI-KK-CCC, which encodes pre-SufI-KK-CCC. The coding region of all plasmid constructs was confirmed by DNA sequencing.

Protein purification

The precursor proteins spTorA-GFP, spTorA12-GFP and spSufI-GFP were expressed from plasmids pTorA-GFP, pTorA12-GFP and pSufI-GFP, respectively, purified under denaturing conditions, and folded by removing urea by dialysis (Bageshwar and Musser, 2007). Pre-SufI was expressed and purified by Ni-NTA chromatography (Bageshwar and Musser, 2007). The pre-SufI mutants were purified in identical fashion. Plasmid pTatABC (Yahr and Wickner, 2001) was used for overexpression of TatA, TatB and TatC under the control of the arabinose promoter (Bageshwar and Musser, 2007). SecB and proOmpA-HisC were purified as described (Liang *et al.*, 2009).

The protein concentrations of all Tat substrates were quantified by SDS-PAGE using bovine serum albumin (BSA) as the standard. Spot intensities after Coomassie Blue staining were determined with a PhosphorImager (model FX; Bio-Rad Laboratories). SecB and proOmpA concentrations were determined by the BCA method (Pierce) using BSA as a standard.

Isolation of IMVs and the in vitro *transport assay*

Inverted membrane vesicles (IMVs) were obtained from *E. coli* strains MC4100, MC4100ΔTatABCDE and JM109, as described (Bageshwar and Musser, 2007). The MC4100 and JM109 strains included the plasmid pTatABC for overexpression of the Tat machinery, which was induced by 0.7% arabinose. The *in vitro* Tat transport assay was performed as described (Bageshwar and Musser, 2007), with minor modifications. These modifications were a slightly increased pH (pH 8), a decreased IMV concentration ($A_{280} = 2$) and transport was usually initiated by NADH addition instead of by IMV addition. The total protein in IMV preparations was quantified as the A_{280} in 2% SDS. Typical IMV stock solutions had an $A_{280} \approx 50–60$. The inside-out percentage of the IMV preparation was identified as described earlier (Fig. S1) (Bageshwar and Musser, 2007). Most standard transport assays were performed with 90 nM pre-SufI (3.1 pmol in 35 μl). This pre-SufI and IMV concentrations used here yield lower overall transport efficiencies than we reported earlier, but the Western blots are cleaner. Variations on these conditions are indicated in the text or figure captions. Precursor transport was initiated by 4 mM NADH addition, unless otherwise noted. When 4 mM ATP was used, a regenerating system was included (7.1 mM phosphocreatine, 0.29 mg ml^{-1} creatine kinase).

The precursor-membrane binding assay

For precursor-membrane binding studies, IMVs (typically $A_{280} = 2$) and precursor (typically 90 nM) were incubated in a 35 μl reaction volume of high-BSA translocation buffer, pH 8.0 (HB-TB). HB-TB contains a 10-fold higher concentration of BSA (570 μg ml^{-1}) than translocation buffer (TB; 5 mM $MgCl_2$, 50 mM KCl, 200 mM sucrose, 57 μg ml^{-1} BSA, 25 mM MOPS, 25 mM MES, pH 8.0). The high BSA concentration was used to help prevent non-specific binding. Protein LoBind microfuge tubes (1.5 ml, Eppendorf) were effective

for eliminating non-specific binding to the walls of the reaction vessel. The selectivity of the binding reaction conditions is illustrated by the complete absence of precursor in the minus IMV control lanes of Figs 2C, 3B and 7C. After a 10 min incubation at 37°C, the binding reactions were centrifuged at 16 200 *g* at 4°C for 30 min to sediment the IMVs. Supernatants were aspirated away. Pellets were washed with 200 µl HB-TB (without resuspension) and re-centrifuged under the same conditions to remove any residual supernatant and any residual precursor bound non-specifically to the reaction vessel. The wash supernatant was removed by aspiration. When monitoring the effect of pH, urea, KCl and urea + KCl on the binding efficiency of precursor proteins to IMVs, pellets of sedimented IMVs were also washed with 200 µl HB-TB. The pellets were then suspended in 2× Gel Buffer (4% SDS, 10% glycerol, 0.04% bromophenol blue, 0.4% β-mercaptoethanol, 10 M urea and 200 mM Tris, pH 6.8), and incubated in a boiling water bath for 10 min. Samples were pulse centrifuged at 16 000 *g*, and then were resolved by 8% SDS-PAGE for pre-SufI and 10% SDS-PAGE for spSufI-GFP, spTorA-GFP and spTorA12-GFP with known standards. Gels were electroblotted onto PVDF membranes and immunoblotted using appropriate antibodies, as described earlier (Bageshwar and Musser, 2007). To rigorously remove soluble pre-SufI (Fig. 8), IMVs were pre-incubated with the precursor protein as described earlier and sedimented three times through a 1.0 ml 0.7 M sucrose cushion on top of a 10 µl 2.2 M sucrose cushion (both cushions were in TB buffer). IMVs were collected from the cushion interface.

Proteolysis of IMVs

Inverted membrane vesicles were treated with trypsin to digest proteins accessible to the aqueous environment as described earlier (Lorence *et al.*, 1988), with minor modifications. IMVs were diluted with TB buffer (pH 8.0) devoid of BSA to $A_{280} = 10$ (1 ml final volume), and treated with 0.5 mg ml^{-1} trypsin (Sigma) for 200 min at room temperature. Digestions were quenched with 50 µl of 100 mg ml^{-1} egg white trypsin inhibitor (Sigma). The trypsinized IMVs were sedimented and washed once with HB-TB, as described in the previous section.

Hydrophobicity values

We tested six different hydrophobicity scales (Kyte and Doolittle, 1982; Pace, 1995; Wimley and White, 1996) to fit the transport efficiency data in Fig. 4D. The cyclohexane-to-water partition coefficient scale (Radzicka *et al.*, 1988) yielded the best correlation with our data. However, this hydrophobicity scale does not include a value for proline, so this data point is not shown. Because there is no value for proline and proline is present in the pre-SufI signal peptide, the Kyte and Doolittle scale (Kyte and Doolittle, 1982) was used for Fig. 4E. The Kyte and Doolittle scale also yielded a reasonable correlation with the transport efficiency data.

Labelled pre-SufI-IAC

The pre-SufI-IAC precursor protein was labelled with biotin and Atto565 at the single C-terminal cysteine as follows. Pre-SufI-IAC was incubated with a 10-fold molar excess of *tris*[2-carboxyethylphosphine] hydrochloride for 10 min (to reduce any disulfides), and then with a 10-fold molar excess of Atto565 maleimide (Sigma) or with 40-fold molar excess of *N*-(3-maleimidyl propionyl)biocytin (Invitrogen) for 15 min (dark, room temperature). Reactions were quenched with 10 mM β-mercaptoethanol, and purified by Ni-NTA chromatography. Labelled proteins were mixed with 1 ml of Ni-NTA Superflow resin (Qiagen) pre-equilibrated with 10 mM Tris, 250 mM NaCl, 20 mM imidazole, pH 8.0. The resin was then loaded onto a 10 × 1 cm column and sequentially washed with: (i) 50 ml of 10 mM Tris-HCl, 1 M NaCl, 20 mM imidazole, pH 8.0; (ii) 20 ml of 100 mM NaCl and 10 mM imidazole, pH 8.0; and (iii) 5 ml of 100 mM NaCl, 10 mM imidazole, 50% glycerol, pH 8.0. The labelled precursor was eluted (0.2 ml fractions) with 100 mM NaCl, 250 mM imidazole, 50% glycerol, pH 8.0, and stored at –80°C. Biotinylated protein was detected on blots with avidin-HRP and chemiluminescence (Harlow and Lane, 1999). Fluorescent proteins were detected by direct in-gel fluorescence imaging using a model FX PhosphorImager (Bio-Rad Laboratories).

Data analysis

All errors are standard deviations. Comparisons of different conditions within each figure panel utilized the same IMV preparation(s). Values compared between panels may be different due to different IMV preparations.

Acknowledgements

We thank T.L. Yahr for pET-SufI, pTatABC, and the TatA, TatB, TatC and SufI antibodies; T.L. Yahr and W. Wickner for ptrcOmp9; A. Driessen for pHKSB366; C. Robinson for pJDT1; T. Palmer for MC4100 and MC4100ΔTatABCDE; and Meng Chen and Kelly Soltysiak for technical assistance. This work was supported by the National Institutes of Health (GM065534) and the Welch Foundation (BE-1541).

References

Alami, M., Luke, I., Deitermann, S., Eisner, G., Koch, H.G., Brunner, J., and Muller, M. (2003) Differential interactions between a twin-arginine signal peptide and its translocase in *Escherichia coli*. *Mol Cell* **12:** 937–946.

Bageshwar, U.K., and Musser, S.M. (2007) Two electrical potential-dependent steps are required for transport by the *Escherichia coli* Tat machinery. *J Cell Biol* **179:** 87–99.

Barrett, C.M., Ray, N., Thomas, J.D., Robinson, C., and Bolhuis, A. (2003) Quantitative export of a reporter protein, GFP, by the twin-arginine translocation pathway in *Escherichia coli*. *Biochem Biophys Res Commun* **304:** 279–284.

Beck, D.A., Bennion, B.J., Alonso, D.O., and Daggett, V. (2007) Simulations of macromolecules in protective and denaturing osmolytes: properties of mixed solvent systems and their effects on water and protein structure and dynamics. *Methods Enzymol* **428:** 373–396.

Bendtsen, J.D., Nielsen, H., Widdick, D., Palmer, T., and Brunak, S. (2005) Prediction of twin-arginine signal peptides. *BMC Bioinformatics* **6:** 167.

Berks, B.C. (1996) A common export pathway for proteins binding complex redox cofactors? *Mol Microbiol* **22:** 393–404.

Berks, B.C., Palmer, T., and Sargent, F. (2003) The Tat protein translocation pathway and its role in microbial physiology. *Adv Microbiol Physiol* **47:** 187–254.

Berks, B.C., Palmer, T., and Sargent, F. (2005) Protein targeting by the bacterial twin-arginine translocation (Tat) pathway. *Curr Opin Microbiol* **8:** 174–181.

Bolhuis, A., Mathers, J.E., Thomas, J.D., Barrett, C.M.L., and Robinson, C. (2001) TatB and TatC form a functional and structural unit of the twin-arginine translocase from *Escherichia coli*. *J Biol Chem* **276:** 20213–20219.

Brüser, T., and Sanders, C. (2003) An alternative model of the twin arginine translocation system. *Microbiol Res* **158:** 7–17.

Brüser, T., Yano, T., Brune, D.C., and Daldal, F. (2003) Membrane targeting of a folded and cofactor-containing protein. *Eur J Biochem* **270:** 1211–1221.

Casadaban, M.J., and Cohen, S.N. (1979) Lactose genes fused to exogenous promoters in one step using a Mu-lac bacteriophage: in vivo probe for transcriptional control sequences. *Proc Natl Acad Sci USA* **76:** 4530–4533.

Chaddock, A.M., Mant, A., Karnauchov, I., Brink, S., Herrmann, R.G., Klosgen, R.B., and Robinson, C. (1995) A new type of signal peptide: central role of a twin-arginine motif in transfer signals for the delta pH-dependent thylakoidal protein translocase. *EMBO J* **14:** 2715–2722.

Cline, K., and Mori, H. (2001) Thylakoid ΔpH-dependent precursor proteins bind to a cpTatC-Hcf106 complex before Tha4-dependent transport. *J Cell Biol* **154:** 719–729.

Cristóbal, S., de Gier, J.W., Nielsen, H., and von Heijne, G. (1999) Competition between Sec- and TAT-dependent protein translocation in *Escherichia coli*. *EMBO J* **18:** 2982–2990.

Dabney-Smith, C., Mori, H., and Cline, K. (2006) Oligomers of Tha4 organize at the thylakoid Tat translocase during protein transport. *J Biol Chem* **281:** 5476–5483.

De Leeuw, E., Porcelli, I., Sargent, F., Palmer, T., and Berks, B.C. (2001) Membrane interactions and self association of the TatA and TatB components of the twin-arginine translocation pathway. *FEBS Lett* **506:** 143–148.

DeLisa, M.P., Lee, P., Palmer, T., and Georgiou, G. (2004) Phage shock protein PspA of *Escherichia coli* relieves saturation of protein export via the Tat pathway. *J Bacteriol* **186:** 366–373.

Driessen, A.J., and Nouwen, N. (2008) Protein translocation across the bacterial cytoplasmic membrane. *Annu Rev Biochem* **77:** 643–667.

Dubini, A., and Sargent, F. (2003) Assembly of Tat-dependent [NiFe] hydrogenases: identification of precursor-binding accessory proteins. *FEBS Lett* **549:** 141–146.

Gérard, F., and Cline, K. (2006) Efficient twin arginine translocation (Tat) pathway transport of a precursor protein covalently anchored to its initial cpTatC binding site. *J Biol Chem* **281:** 6130–6135.

Gérard, F., and Cline, K. (2007) The thylakoid proton gradient promotes an advanced stage of signal peptide binding deep within the Tat pathway receptor complex. *J Biol Chem* **282:** 5263–5272.

Gohlke, U., Pullan, L., McDevitt, C.A., Porcelli, I., de Leeuw, E., Palmer, T., *et al.* (2005) The TatA component of the twin-arginine protein transport system forms channel complexes of variable diameter. *Proc Natl Acad Sci USA* **102:** 10482–10486.

Graubner, W., Schierhorn, A., and Bruser, T. (2007) DnaK plays a pivotal role in Tat targeting of CueO and functions beside SlyD as a general Tat signal binding chaperone. *J Biol Chem* **282:** 7116–7124.

Harlow, E., and Lane, D. (1999) *Using Antibodies: A Laboratory Manual*. New York: Cold Spring Harbor Laboratory Press.

Hinsley, A.P., Stanley, N.R., Palmer, T., and Berks, B.C. (2001) A naturally occurring bacterial Tat signal peptide lacking one of the 'invariant' arginine residues of the consensus targeting motif. *FEBS Lett* **497:** 45–49.

Holzapfel, E., Eisner, G., Alami, M., Barrett, C.M., Buchanan, G., Luke, I., *et al.* (2007) The entire N-terminal half of TatC is involved in twin-arginine precursor binding. *Biochemistry* **46:** 2892–2898.

Holzapfel, E., Moser, M., Schiltz, E., Ueda, T., Betton, J.-M., and Muller, M. (2009) Twin-arginine-dependent translocation of SufI in the absence of cytosolic helper proteins. *Biochemistry* **48:** 5096–5105.

Hou, B., Frielingsdorf, S., and Klösgen, R.B. (2006) Unassisted membrane insertion as the initial step in ΔpH/Tat-dependent protein transport. *J Mol Biol* **355:** 957–967.

Hua, L., Zhou, R., Thirumalai, D., and Berne, B.J. (2008) Urea denaturation by stronger dispersion interactions with proteins than water implies a 2-stage unfolding. *Proc Natl Acad Sci USA* **105:** 16928–16933.

Jack, R.L., Buchanan, G., Dubini, A., Hatzixanthis, K., Palmer, T., and Sargent, F. (2004) Coordinating assembly and export of complex bacterial proteins. *EMBO J* **23:** 3962–3972.

Kyte, J., and Doolittle, R.F. (1982) A simple method for displaying the hydropathic character of a protein. *J Mol Biol* **157:** 105–132.

Li, H., Faury, D., and Morosoli, R. (2006) Impact of amino acid changes in the signal peptide on the secretion of the Tat-dependent xylanase C from *Streptomyces lividans*. *FEMS Microbiol Lett* **255:** 268–274.

Liang, F.-C., Bageshwar, U.K., and Musser, S.M. (2009) Bacterial Sec protein transport is rate-limited by precursor length: a single turnover study. *Mol Biol Cell* **20:** 4256–4266.

Lorence, R.M., Carter, K., Gennis, R.B., Matsushita, K., and Kaback, H.R. (1988) Trypsin proteolysis of the cytochrome *d* complex of *Escherichia coli* selectively inhibits ubiquinol oxidase activity while not affecting N,N,N′,N′-tetramethyl-*p*-phenylenediamine oxidase activity. *J Biol Chem* **263:** 5271–5276.

McDevitt, C.A., Buchanan, G., Sargent, F., Palmer, T., and Berks, B.C. (2006) Subunit composition and in vivo substrate-binding characteristics of *Escherichia coli* Tat protein complexes expressed at native levels. *FEBS J* **273:** 5656–5668.

Maillard, J., Spronk, C.A., Buchanan, G., Lyall, V., Richardson, D.J., Palmer, T., *et al.* (2007) Structural diversity in twin-arginine signal peptide-binding proteins. *Proc Natl Acad Sci USA* **104:** 15641–15646.

Matos, C.F., Robinson, C., and Di Cola, A. (2008) The Tat system proofreads FeS protein substrates and directly initiates the disposal of rejected molecules. *EMBO J* **27:** 2055–2063.

Molik, S., Karnauchov, I., Weidlich, C., Herrmann, R.G., and Klosgen, R.B. (2001) The Rieske Fe/S protein of the cytochrome b_6/f complex in chloroplasts: missing link in the evolution of protein transport pathways in chloroplasts? *J Biol Chem* **276:** 42761–42766.

Musser, S.M., and Theg, S.M. (2000) Characterization of the early steps of OE17 precursor transport by the thylakoid ΔpH/Tat machinery. *Eur J Biochem* **267:** 2588–2598.

Natale, P., Brüser, T., and Driessen, A.J. (2008) Sec- and Tat-mediated protein secretion across the bacterial cytoplasmic membrane – distinct translocases and mechanisms. *Biochim Biophys Acta* **1778:** 1735–1756.

Oresnik, I.J., Ladner, C.L., and Turner, R.J. (2001) Identification of a twin-arginine leader-binding protein. *Mol Microbiol* **40:** 323–331.

Pace, C.N. (1995) Evaluating contribution of hydrogen bonding and hydrophobic bonding to protein folding. *Methods Enzymol* **259:** 538–554.

Panahandeh, S., Maurer, C., Moser, M., Delisa, M.P., and Müller, M. (2008) Following the path of a twin-arginine precursor along the TatABC translocase of *Escherichia coli*. *J Biol Chem* **283:** 33267–33275.

Papish, A.L., Ladner, C.L., and Turner, R.J. (2003) The twin-arginine leader-binding protein, DmsD, interacts with the TatB and TatC subunits of the *Escherichia coli* twin-arginine translocase. *J Biol Chem* **278:** 32501–32506.

Radzicka, A., Pedersen, L., and Wolfenden, R. (1988) Influences of solvent water on protein folding: free energies of solvation of cis and trans peptides are nearly identical. *Biochemistry* **27:** 4538–4541.

Rusch, S.L., and Kendall, D.A. (2007) Interactions that drive Sec-dependent bacterial protein transport. *Biochemistry* **46:** 9665–9673.

Sambrook, J., and Russell, D.W. (2001) *Molecular Cloning: A Laboratory Manual.* Cold Spring Harbor, NY: Cold Spring Harbor Press.

Santini, C.L., Bernadac, A., Zhang, M., Chanal, A., Ize, B., Blanco, C., and Wu, L.F. (2001) Translocation of jellyfish green fluorescent protein via the Tat system of *Escherichia coli* and change of its periplasmic localization in response to osmotic up-shock. *J Biol Chem* **276:** 8159–8164.

Sargent, F. (2007) The twin-arginine transport system: moving folded proteins across membranes. *Biochem Soc Trans* **35:** 835–847.

Sargent, F., Stanley, N.R., Berks, B.C., and Palmer, T. (1999) Sec-independent protein translocation in *Escherichia coli*: a distinct and pivotal role for the TatB protein. *J Biol Chem* **274:** 36073–36082.

Shanmugham, A., Wong Fong Sang, H.W., Bollen, Y.J., and Lill, H. (2006) Membrane binding of twin arginine preproteins as an early step in translocation. *Biochemistry* **45:** 2243–2249.

Stanley, N.R., Palmer, T., and Berks, B.C. (2000) The twin arginine consensus motif of Tat signal peptides is involved in Sec-independent protein targeting in *Escherichia coli*. *J Biol Chem* **275:** 11591–11596.

Studier, F.W., Rosenberg, A.H., Dunn, J.J., and Dubendorff, J.W. (1990) Use of T7 RNA polymerase to direct expression of cloned genes. *Methods Enzymol* **185:** 60–89.

Stumpe, M.C., and Grubmüller, H. (2007) Interaction of urea with amino acids: implications for urea-induced protein denaturation. *J Am Chem Soc* **129:** 16126–16131.

Stumpe, M.C., and Grubmüller, H. (2008) Polar or apolar – the role of polarity for urea-induced protein denaturation. *PLoS Comput Biol* **4:** e1000221.

Tarry, M.J., Schäfer, E., Chen, S., Buchanan, G., Greene, N.P., and Lea, S.M., *et al.* (2009) Structural analysis of substrate binding by the TatBC component of the twin-arginine protein transport system. *Proc Natl Acad Sci USA* **106:** 13284–13289.

Thomas, J.D., Daniel, R.A., Errington, J., and Robinson, C. (2001) Export of active green fluorescent protein to the periplasm by the twin-arginine translocase (Tat) pathway in *Escherichia coli*. *Mol Microbiol* **39:** 47–53.

Wexler, M., Sargent, F., Jack, R.L., Stanley, N.R., Bogsch, E.G., Robinson, C., *et al.* (2000) TatD is a cytoplasmic protein with DNase activity. No requirement for TatD family proteins in Sec-independent protein export. *J Biol Chem* **275:** 16717–16722.

Wimley, W.C., and White, S.H. (1996) Experimentally determined hydrophobicity scale for proteins at membrane interfaces. *Nat Struct Biol* **3:** 842–848.

Yahr, T.L., and Wickner, W.T. (2001) Functional reconstitution of bacterial Tat translocation in vitro. *EMBO J* **20:** 2472–2479.

Yanisch-Perron, C., Vieira, J., and Messing, J. (1985) Improved M13 phage cloning vectors and host strains: nucleotide sequences of the M13mp18 and pUC19 vectors. *Gene* **33:** 103–119.

Supporting information

Additional supporting information may be found in the online version of this article.

Please note: Wiley-Blackwell are not responsible for the content or functionality of any supporting materials supplied by the authors. Any queries (other than missing material) should be directed to the corresponding author for the article.